Geometric phase of optical rotators

Enrique J. Galvez and Chris D. Holmes*

Department of Physics and Astronomy, Colgate University, Hamilton, New York 13346

We describe the rotation of images by means of optical beam steering with use of the concept of geometric phase. The discussion is concentrated on systems composed of discrete reflections but can be generalized to refractive steering systems. Geometric phase reduces the analysis of image rotation to simple geometric constructions and the calculation of areas on a sphere. The analysis also applies to the rotation of linear polarization of the light with ideal mirrors. © 1999 Optical Society of America [S0740-3232(99)01008-X]

OCIS codes: 350.1370, 220.0220, 080.2740, 110.2960.

1. INTRODUCTION

Reflection of images is one of the oldest problems studied in classical optics. Currently a large number of mirror and prism systems are available for the manipulation of images.[1,2] Simple graphical constructions are sufficient for understanding the operation of systems in which the incoming and outgoing light directions are parallel or orthogonal. For other, more general cases one has to resort to matrix methods to find the properties (e.g., orientation) of the final image.[3] Despite the level of maturity of this topic, in recent years the application of differential geometry concepts to physical systems has brought new light to this problem, among many others. The topic of this paper is to present the application of this new concept of geometric phase to the design and analysis of optical rotators. This new method reduces the analysis to a geometrical construction, for which computation and visualization are much simpler than is the case with other analytical methods. An interesting aspect of this application is that the concepts of geometric phase apply to the polarization of the light as well as to images.

Geometric phase was first introduced by Berry in quantum systems.[4] The concept had a profound effect, because it highlighted a serious oversight in quantum mechanics: When a system undergoes cyclic changes in parameter space, it acquires a nonintegrable phase (geometric phase), also known as Berry's phase. The manifestation of geometric phase in optics, in the context of quantum mechanics, was first investigated by Chiao and co-workers.[5] Its presence in image rotation was proposed by Segev *et al.*[6] but was not developed explicitly for application to imaging systems. Another important manifestation in optics, known about much earlier and now referred to as the Pancharatnam phase, is the phase that the light acquires after undergoing changes in its polarization state.[7,8] Although the geometric phase was initially believed to be a purely quantum phenomenon, its strong presence in classical mechanics is now widely accepted. Likewise, initial restrictions of adiabaticity[9] and the requirement of a closed path have been relaxed.[10]

2. GEOMETRIC PHASE OF COILED OPTICS

The origin of the geometric phase can best be understood in terms of differential geometry. A geometric phase is a consequence of the parallel transport in a curved topology. This topology is defined by the parameters of the system. In the case of coiled optics, where the light follows a three-dimensional path, the parameters of the system are the coordinates of the propagation vector. In systems with n mirrors, the helicity vector, rather than the propagation vector, defines the state of the system.[11] This is because the helicity accounts for the inversion introduced by each mirror reflection, hereafter called mirror inversion. The helicity vector after the nth reflection is defined as

$$\tilde{\mathbf{k}}_n = (-1)^n \mathbf{k}_n, \tag{1}$$

where $\mathbf{k}_n$ is the propagation vector after the nth reflection. If the helicity vector of the light is mapped onto a unit sphere, as the light follows its path through the imaging system the point on the sphere representing the helicity vector describes a curve, C, on the sphere. In the case of discrete reflections by mirrors, C is formed by connecting with geodesics the discrete positions of the helicities mapped onto the sphere. Since the image plane is perpendicular to the helicity vector (i.e., is tangent to the sphere), a three-dimensional light path will parallel transport the image plane along C and therefore produce a rotation of the image. Differential geometry provides the proper formalism for the description of this rotation by means of the angle accrued by the tangent to C along the path.[12,13] When C is closed, the angle can be simply obtained, with the Gauss–Bonnet theorem as the area enclosed by C.[13,14] This area is also equivalent to the solid angle described by the helicity vector in configuration space. A geometric phase also exists in the case of open curves, and a "closing" geodesic allows the application of the Gauss–Bonnet theorem.[12] However, care should be taken in defining a way to compare input and output images, as will be shown below.

The new simplification that geometric phase brings to the analysis of optical rotation is this reduction of the image rotation to the calculation of a spherical area in the unit helicity-vector sphere. In the following sections, we will discuss the application of the geometric-phase method to reflective optical rotators. The paper is divided into different cases, depending on whether the number of reflections is even or odd and on whether C is closed or not. The notation used is the following: $\tilde{\mathbf{k}}_i$ denotes the helicity vector after the ith steering of the optical beam, with $\tilde{\mathbf{k}}_0$ representing the initial helicity. The final helicity is denoted in a general way by $\tilde{\mathbf{k}}_f$. The subindexes for the propagation vector follow the same convention.

The discussions in this article can be generalized to refractive systems as well. In the case of optical steering by refraction, the relation between the helicity and propagation vectors (parallel or antiparallel) remains the same after the steering, as opposed to the case of the reflective steering of images, in which the relation changes after each reflection. Thus for purely refractive systems such as coherent image bundles, the propagation vector is sufficient to describe the geometric phase of the system.

3. CASE 1: EVEN NUMBER OF REFLECTIONS

A. Case 1(a): $\tilde{\mathbf{k}}_f = \tilde{\mathbf{k}}_0$

Case 1(a), $\tilde{\mathbf{k}}_f = \tilde{\mathbf{k}}_0$, is the simplest but most important case. The input and output beams are parallel, and the final image is not mirror inverted. Here the geometric phase is manifested in its purest form: The image rotation depends only on the path of the light. That is, it is independent of the orientation of the incident image relative to the optical system. This type of optical rotator is also referred to as a pure rotator.

Consider the system shown in Fig. 1(a). The unit-norm propagation vectors for this geometry are $\mathbf{k}_0 = (0, 1, 0)$, $\mathbf{k}_1 = (1, 0, 0)$, $\mathbf{k}_2 = (0, 0, 1)$, $\mathbf{k}_3 = (-\sin\theta, -\cos\theta, 0)$, and $\mathbf{k}_4 = \mathbf{k}_0$. The corresponding $\tilde{\mathbf{k}}$ sphere is shown in Fig. 1(b). The points in the sphere corresponding to the mapping of the helicity vector $\tilde{\mathbf{k}}_n$ are denoted for simplicity by $\tilde{\mathbf{n}}$. From Fig. 1(b) it can be seen that the spherical area enclosed by C (or the solid angle Ω described by $\tilde{\mathbf{k}}$) is given by $90° + \theta$. We verified this relationship experimentally by sending the light from a slide projector through the optical system described schematically by Fig. 1(a). The reflectors were 4 in $\times$ 4 in frontsurface Al mirrors aligned into position with intersecting He–Ne and red-diode laser beams with a diameter of ~1 mm. The rotation angle ϕ was measured with a protractor directly on a screen, where the overlapping original and rotated images of a pattern were projected. Figure 2 shows a comparison of ϕ as a function of the computed spherical area. The squares correspond to the geometry of Fig. 1(a). The triangle corresponds to a measurement where $\mathbf{k}_3$ was off the horizontal plane: $\mathbf{k}_3 = (3, 4, 2)/\sqrt{29}$. The errors for each data point are of the order of 1° owing to the uncertainties in the position of the mirrors, which were caused by the finite width of the laser beams used to align them.

The sense of the rotation of the image was consistent with the sense of the trajectory through C as seen from the center of the sphere. In our convention, positive signs correspond to clockwise rotations. From this, one would expect that a curve C in the form of a figure eight would give a geometric phase that is the difference in the areas of the two figure-eight lobes. Indeed, the circle in Fig. 2 corresponds to the case in which $\mathbf{k}_0 = (0, 1, 0)$, $\mathbf{k}_1 = (5, 0, 3)/\sqrt{34}$, $\mathbf{k}_2 = (0, 0, 1)$, $\mathbf{k}_3 = (3, 4, 0)/5$, and $\mathbf{k}_4 = \mathbf{k}_0$. The optical apparatus and the spherical construction are shown in Fig. 3. The measured rotation was $-22.3°$. The calculated difference in the two areas is $-22.2°$, and their sum is $84.1°$.

It is straightforward to verify that the Porro, Abbe, Abbe's modification of Porro, Leman, Carl–Zeiss, Hensolt, and Goerz prism systems,[15] which fall under this category, rotate the image by 180°. We shall discuss explicitly two interesting variations of popular systems, which we call the variable-angle Porro and consecutive Dove systems. Both are important because the angle of rotation of the image is variable. The first system consists of two right-angle prisms arranged as in the Porro system, but the angle between the two prisms is variable [see Fig. 4(a)]. In the first prism the $\tilde{\mathbf{k}}$ vector describes a great semicircle, and in the second one it describes another great semicircle (in general, in a different plane) that closes C. The planes of the two great semicircles form
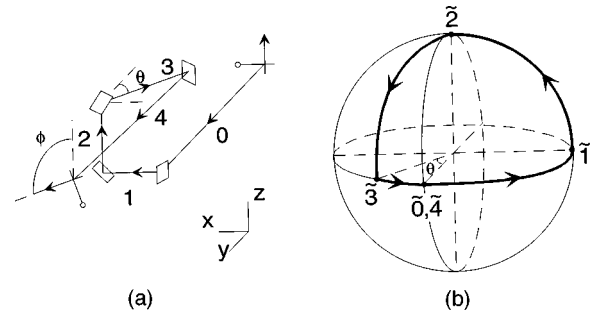

Fig. 1. System to test the case of cyclic geometric phase with an even number of reflections: (a) experimental arrangement of mirrors with $\mathbf{k}_0 = (0, 1, 0)$, $\mathbf{k}_1 = (1, 0, 0)$, $\mathbf{k}_2 = (0, 0, 1)$, $\mathbf{k}_3 = (-\sin\theta, -\cos\theta, 0)$, and $\mathbf{k}_4 = \mathbf{k}_0$ and (b) the $\tilde{\mathbf{k}}$-sphere construction that predicts $\phi = 90° + \theta$.

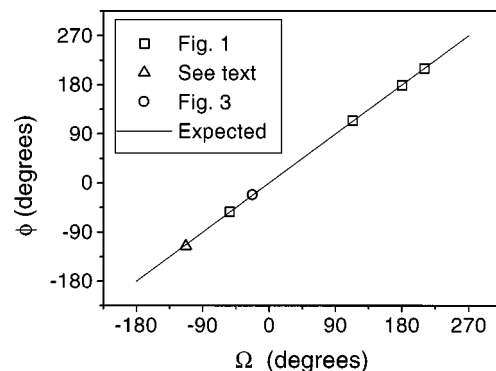Fig. 2. Measurements of image rotation as a function of the solid angle Ω (the calculated area in the $\tilde{\mathbf{k}}$ sphere) for case 1(a) (see text).
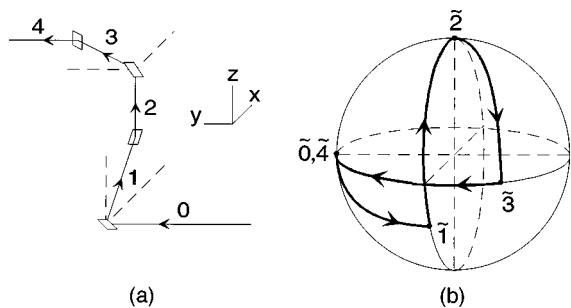
Fig. 3. Optical system to verify the predictions of a geometric phase for a figure-eight path in the helicity sphere: (a) experimental arrangement of mirrors with $\mathbf{k}_0 = (0, 1, 0)$, $\mathbf{k}_1 = (5, 0, 3)/(34)^{1/2}$, $\mathbf{k}_2 = (0, 0, 1)$, $\mathbf{k}_3 = (3, 4, 0)/5$, and $\mathbf{k}_4 = \mathbf{k}_0$ and (b) the corresponding $\tilde{\mathbf{k}}$-sphere construction.
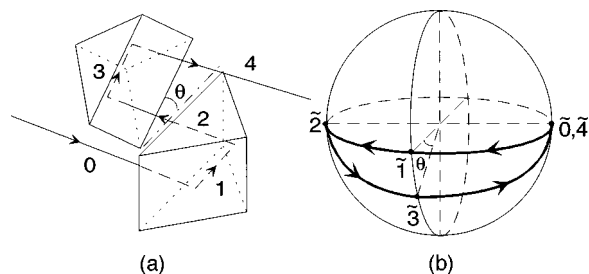

Fig. 4. Analysis of the geometric phase of the variable-angle Porro system: (a) prism arrangement and (b) the corresponding $\tilde{\mathbf{k}}$-sphere construction that predicts $\phi = 2\theta$.

the same angle θ between the hypotenuses of the two prisms. The curve C resembles a tangerine slice, shown in Fig. 4(b), with an enclosed spherical area of 2θ. The 180° rotation needed in binoculars is achieved by setting $\theta = 90°$.

The consecutive Dove system, shown in Fig. 5(a), consists of two Dove prisms in series, where the angle between the verticals of the two is variable. This is an interesting system because each Dove prism has only one reflection. As a consequence, in each of them the $\tilde{\mathbf{k}}$ vector describes a great semicircle as in the case of the variable-angle Porro system. Note that here we have the peculiar situation that $\tilde{\mathbf{k}}_j = -\mathbf{k}_j$ for $j = 2, 3, 4$ because the refractions between the two reflections do not alter the relationship between the helicity and the propagation vectors. The angle between the planes of the two great semicircles is the same angle θ formed by the verticals of the two prisms, as shown in Fig. 5(a). The corresponding spherical area is given by $360° - 2\theta$, as shown in Fig. 5(b). Indeed, a 180° rotator such as this one with $\theta = 90°$ is described in Ref. 16. A similar effect is obtained with reversion prisms. More details and measurements on the variable-angle Porro and consecutive Dove system will be given elsewhere.

Since this analysis also applies to the polarization of the light, these arrangements can be used for making pure polarization rotators, provided that linear-polarization-preserving reflectors are used.

B. Case 1(b): $\tilde{\mathbf{k}}_f \neq \tilde{\mathbf{k}}_0$
When the input and output helicity vectors are not parallel, C is open. In such a case the parallel-transport con-

struction and the application of the Gauss–Bonnet theorem can still be made by connecting the input and output points in the $\tilde{\mathbf{k}}$ sphere with a geodesic.[10,12] Although a geometric phase still exists for out-of-plane light paths, the interpretation of the spherical area obtained when C is forced to be closed is now more subtle. This is because in order to obtain a measure of the rotation, we must compare the final and initial images of light beams going in different directions. We have verified experimentally that except for the case in which the input and output helicities are antiparallel, the angle of rotation is indeed the area obtained when C is closed with a (unique) geodesic. We can compare the input and output images by transporting without mirror inversion the final image along the geodesic that closes C. Physically, this is equivalent to steering the beam in the direction of $\tilde{\mathbf{k}}_0$ with a nonmirror-inverting in-plane steering system, such as a coherent fiber bundle or an even set of reflections. In our experiment we used the four-mirror arrangement of Fig. 6(a). We kept the direction of the output confined to the horizontal plane and compared the input and output images by measuring their orientations relative to the vertical. The $\tilde{\mathbf{k}}$-sphere construction is shown in Fig. 6(b), and the results of our measurements are shown in Fig. 6(c).

Two popular systems under this case are the Amici and Schmidt prisms.[15] The Amici prism steers the beam of light 90° with a "rooftop." If the normals to the reflecting faces of the prism are $\mathbf{n}_1 = (-1/\sqrt{2}, -1/2, -1/2)$ and $\mathbf{n}_2 = (1/\sqrt{2}, -1/2, -1/2)$, with $\mathbf{k}_0 = (0, 1, 0)$, then $\mathbf{k}_1 = (-1/\sqrt{2}, 1/2, -1/2)$ and $\mathbf{k}_2 = (0, 0, -1)$. It can be calculated that C forms a spherical triangle of area 180°. Similarly, the Schmidt prism rotates the image by 180°, with a steering angle of 45°. Other prism systems such as the Penta and Wollaston prisms have a zero rotation angle because they involve in-plane beam paths.

An important special case within this subdivision is when $\tilde{\mathbf{k}}_f = -\tilde{\mathbf{k}}_0$, for which the closing geodesic is a great semicircle. This is a case in which the closing geodesic is not unique. One way to compare input and output images consistently is to have a horizontal closing geodesic. The enclosed area is consistent with the image rotation that is seen after the output beam is steered horizontally without mirror inversion. Although this prescription explains the observed rotation, it is not clear that a geometric phase is really present in this case, because the final $\mathbf{k}$ vector may be arrived at by either an in-plane or an out-of-plane path.
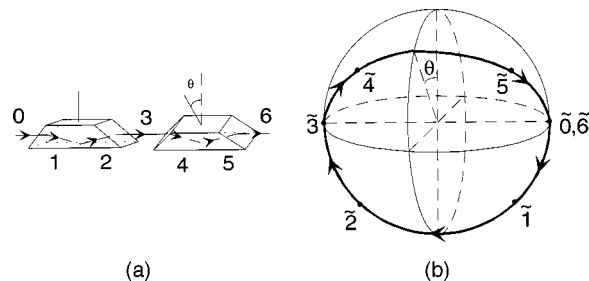

Fig. 5. Analysis of the geometric phase of the consecutive Dove system: (a) prism arrangement and (b) the corresponding $\tilde{\mathbf{k}}$-sphere construction that predicts $\phi = 360° - 2\theta$.
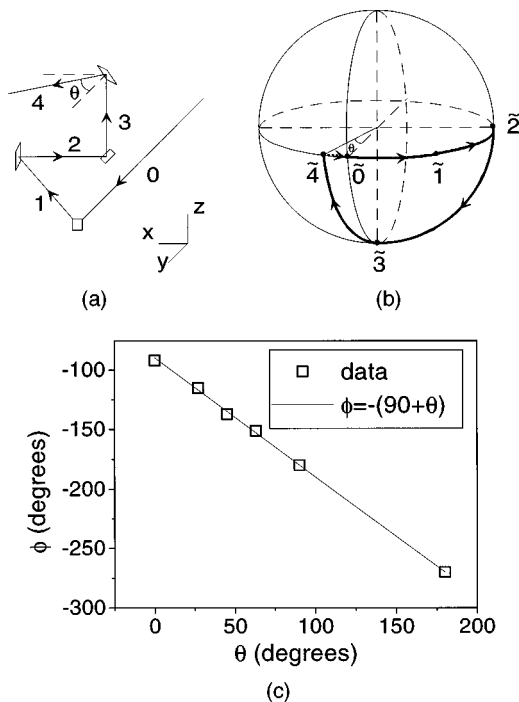
Fig. 6. System to test the case of noncyclic geometric phase with an even number of reflections: (a) experimental arrangement of mirrors with $\mathbf{k}_0 = (0, 1, 0)$, $\mathbf{k}_1 = (-1, -1, 0)/2^{1/2}$, $\mathbf{k}_2 = (-1, 0, 0)$, $\mathbf{k}_3 = (0, 0, 1)$, and $\mathbf{k}_4 = (\sin\theta, \cos\theta, 0)$, (b) the $\tilde{\mathbf{k}}$-sphere construction, with the (dotted) closing geodesic that predicts $\phi = -(90° + \theta)$, and (c) experimental results.

4. CASE 2: ODD NUMBER OF REFLECTIONS

All the systems that lie within this case produce a rotation plus a mirror-inverted image. The constructions described below account only for the rotation of the image. Thus we must perform a mirror inversion on the final image in order to compare it with the input. We can account for the effect of mirror inversion on linear polarization by changing the sign of the geometric phase.

A. Case 2(a): $\tilde{\mathbf{k}}_f = \tilde{\mathbf{k}}_0$

Since we have an odd number of reflections, the case $\tilde{\mathbf{k}}_f = \tilde{\mathbf{k}}_0$ implies that the input and output propagation vectors are antiparallel. However, since C is closed there is no ambiguity, and such a system is a pure rotator. This case has been verified experimentally for polarization of light.[17] An interesting example of this case is the corner-cube retroreflector. If the normals to the planes of the cube are $\mathbf{n}_1 = (0, 1, 0)$, $\mathbf{n}_2 = (1, 0, 0)$, and $\mathbf{n}_3 = (0, 0, 1)$ and if $\mathbf{k}_0 = (x, y, z)$ [with $(x^2 + y^2 + z^2)^{1/2} = 1$], then $\mathbf{k}_1 = (x, -y, z)$, $\mathbf{k}_2 = (-x, -y, z)$, and $\mathbf{k}_3 = (-x, -y, -z)$. The area formed by the resulting spherical triangle is 180° (always!). An interesting application of this is that a corner cube made of ideal mirrors (e.g., metallic mirrors with far-infrared radiation) preserves the plane of linear polarization. A Michelson interferometer or a laser cavity with these type of mirrors will be alignment free and in addition will preserve linear polarization.

B. Case 2(b): $\tilde{\mathbf{k}}_f \neq \tilde{\mathbf{k}}_0$

For the cases in which the $\tilde{\mathbf{k}}$ vectors are not antiparallel, the same prescription as for case 1(b) applies. If we use a reflection to simulate the closing geodesic, the C-closing reflection makes the image not mirror inverted, and it can be compared directly with the input image. This case becomes identical to case 1(b).

There are important systems of odd number of reflections for which $\tilde{\mathbf{k}}$ vectors are antiparallel (i.e., $\tilde{\mathbf{k}}_f = -\tilde{\mathbf{k}}_0$). This particular case represents an important class of pseudorotators, for which the amount of rotation depends on the orientation of the input. Thus the vertical axis for the construction described below is defined by the vertical of the incident image for image rotation or by the incident plane of linear polarization for polarization rotation. A popular pseudorotator is the Dove prism.[2] The prescription here is, similarly to case 1(b), to close C with a noninverting horizontal geodesic. In this case the observed rotation is consistent with the area of the closed C. If the prism is tilted by an angle θ, then $\phi = 180° - 2\theta$, as shown in Fig. 7. Pseudorotators are associated not only with an odd number of reflections when the input and output propagation vectors are parallel but also with systems with an even number of reflections when the input and output propagation vectors are antiparallel (e.g., when a right-angle prism is used as a retroreflector).

As a final example, we present a popular system of three orthogonal reflections that is used to rotate the polarization of laser beams by 90° (see, for example, p. 23 of Ref. 8). A common misconception is that this system always rotates the polarization by 90°. However, here we show that this is not the case. A sketch of such a system in a general setting is shown in Fig. 8. Following our convention for pseudorotators, let us assume that the input linear polarization is aligned with the vertical. If θ is as defined in Fig. 8(a), then from the $\tilde{\mathbf{k}}$-sphere construction shown in Fig. 8(b) and mirror inversion, the polarization-rotation angle is $-(90° + 2\theta)$. To transform the input linear polarization to an orthogonal orientation, we must have $\theta = m\pi/2$, with m integer, which is consistent with requiring that the input polarization be parallel or perpendicular to the plane of incidence of the first mirror. Interestingly, ordinary mirrors in the visible do not conserve linear polarization, thus preventing a verification of the above relation and perpetuating the misconception. We have verified this relation experi-
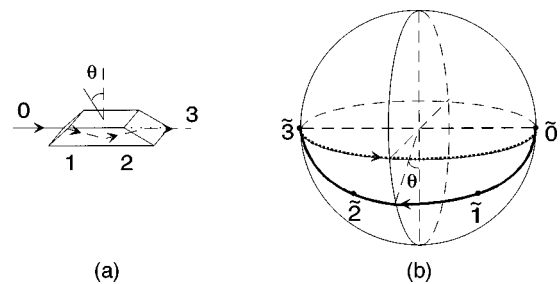

Fig. 7. Analysis of the geometric phase of the Dove prism: (a) prism schematic and (b) the corresponding $\tilde{\mathbf{k}}$-sphere construction, with the (dotted) closing geodesic that predicts $\phi = 180° - 2\theta$.
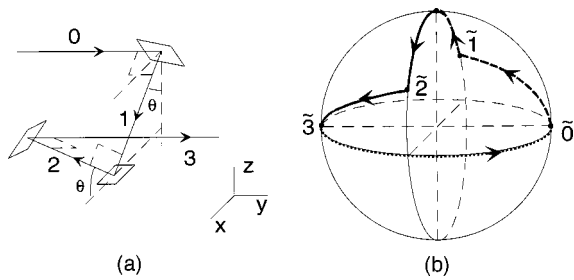
Fig. 8. Analysis of the geometric phase of a popular polarization rotator made of orthogonal reflections, a noncyclic case with an odd number of mirrors and antiparallel input and output $\tilde{\mathbf{k}}$ vectors: (a) mirror schematic with $\mathbf{k}_0 = (0, 1, 0)$, $\mathbf{k}_1 = (\sin \theta, 0, -\cos \theta)$, $\mathbf{k}_2 = (\cos \theta, 0, \sin \theta)$, and $\mathbf{k}_3 = \mathbf{k}_0$ and (b) the corresponding $\tilde{\mathbf{k}}$-sphere construction, with the (dotted) closing geodesic that predicts $\phi = 90° + 2\theta$.
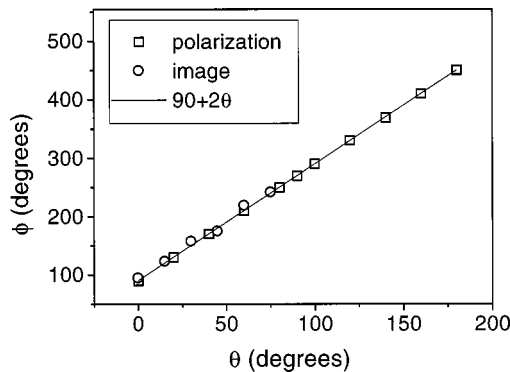

Fig. 9. Measurement of the polarization (squares) and image (circle) rotation for the mirror arrangement of Fig. 8(a). The results are consistent with the results of the $\tilde{\mathbf{k}}$-sphere construction of Fig. 8(b).

mentally for images and polarization rotation. Figure 9 shows the measurements of the counterclockwise (owing to mirror inversion) polarization rotation (squares) and the clockwise image rotation (circles) as a function of the input orientation θ. The polarization-rotation measurements were done with a He–Ne laser and commercial dielectric mirrors.[18] Unlike pure rotators, with which the image and the linear-polarization plane get rotated by the same amount, in pseudorotators such as this one the rotation for each one may be different.

5. SUMMARY AND CONCLUSIONS

In summary, we discuss here the analysis of all cases of rotation of images by means of steering reflections or refractions, using the concept of geometric phase. The analysis is a useful and simpler alternative to analytical methods for finding the rotation of images in complex light-steering systems. We find that systems of even (odd) number of mirrors in which the input and output beams are parallel (antiparallel) are pure rotators. Conversely, systems of even (odd) number of mirrors with antiparallel (parallel) input and output beams are pseudorotators. Two pseudorotators in a series produce a pure rotator; the rotation angle (geometric phase) is determined by the relative orientation of the two rotators. Examples of the latter are the variable-angle Porro and the

consecutive Dove prism systems discussed above. That the concepts of geometric phase apply identically to light polarization as well as to image rotation has important applications for polarization rotators with polarization-preserving steering components. Finally, regardless of whether pseudorotators possess a geometric phase, here we show that the $\tilde{\mathbf{k}}$-sphere construction can be used to determine the rotation they impart to images and polarization.

ACKNOWLEDGMENTS

*Permanent address: Norwich High School, Norwich, New York 13815.

REFERENCES AND NOTES

1. *Optical Design*, MIL-HDBK-141, U.S. Defense Supply Agency Rep. 13-113-52 (Washington, D.C., 1962).
2. D. W. Swift, "Image rotation devices—a comparative study," Opt. Laser Technol. , 175–188 (August 1972).
3. R. E. Hopkins, "Mirror and prism systems," Appl. Opt. Opt. Eng. **3**, 269–308 (1965).
4. M. V. Berry, "Quantum phase factors accompanying adiabatic changes," Proc. R. Soc. London Ser. A **392**, 45–57 (1984).
5. R. Y. Chiao and Y.-S. Wu, "Manifestations of Berry's topological phase for the photon," Phys. Rev. Lett. **57**, 933–936 (1986); A. Tomita and R. Y. Chiao, "Observation of Berry's topological phase by use of an optical fiber," Phys. Rev. Lett. **57**, 937–940 (1986).
6. M. Segev, R. Solomon, and A. Yariv, "Manifestation of Berry's phase in image-bearing optical beams," Phys. Rev. Lett. **69**, 590–592 (1992).
7. R. Bhandari and J. Samuel, "Observation of topological phase by use of a laser interferometer," Phys. Rev. Lett. **13**, 1211–1213 (1988).
8. R. Bhandari, "Polarization of light and topological phases," Phys. Rep. **281**, 1–64 (1997).
9. Y. Aharonov and J. Anandan, "Phase change during a cyclic quantum evolution," Phys. Rev. Lett. **58**, 1593–1596 (1987).
10. J. Samuel and R. Bhandari, "General setting for Berry's phase," Phys. Rev. Lett. **60**, 2339–2342 (1988).
11. M. Kitano, T. Yabuzaki, and T. Ogawa, "Comment on 'Observation of Berry's topological phase by use of an optical fiber'," Phys. Rev. Lett. **58**, 523 (1987).
12. F. D. M. Haldane, "Path dependence of the geometric rotation of polarization in optical fibers," Opt. Lett. **11**, 730–732 (1986).
13. J. Segert, "Photon's Berry's phase as a classical topological effect," Phys. Rev. A **36**, 10–15 (1987).
14. L. H. Ryder, "The optical Berry phase and the Gauss–Bonnet theorem," Eur. J. Phys. **12**, 15–18 (1991).
15. W. J. Smith, "Image formation: geometrical and physical optics," in *Handbook of Optics*, W. G. Driscoll and W. Vaughan, eds. (McGraw-Hill, New York, 1978), pp. 2-41–2-51.
16. A. Gleichen, *The Theory of Modern Optical Instruments* (His Majesty's Stationery Office, London, 1921).
17. E. J. Galvez and P. M. Koch, "Use of four mirrors to rotate linear polarization but preserve input–output collinearity. II," J. Opt. Soc. Am. A **14**, 3410–3414 (1997).
18. Empirically we found a commercial dielectric mirror, New Focus model 5102, that conserved linear polarization and had high s and p polarization reflectances for an angle of incidence of 45° at 633 nm.